SUPPLEMENTARY FIGURES
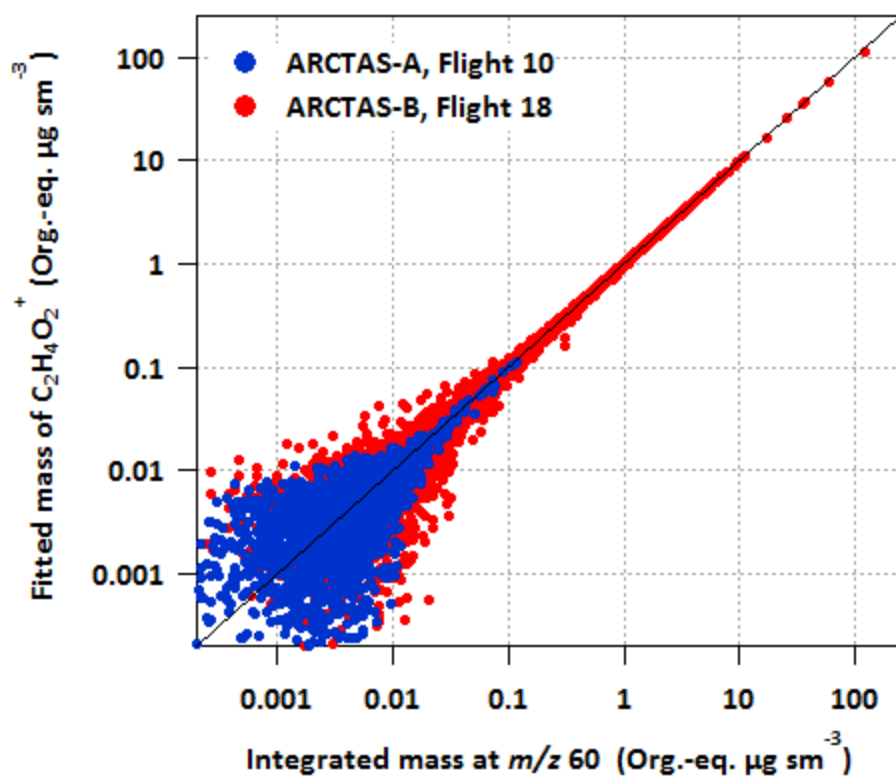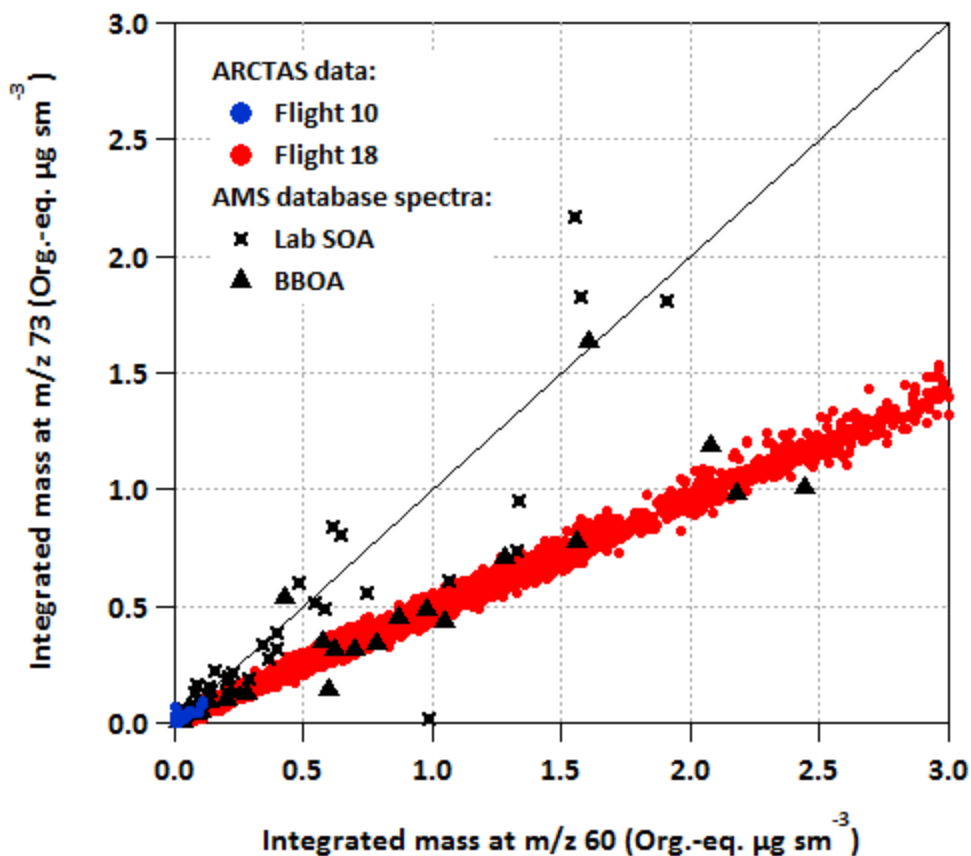

Figure S1. Scatter plot showing the correlation between the integrated organic-equivalent mass concentration at AMS m/z 60 and the signal of the $C_2H_4O_2^+$ ion (from high-resolution peak fitting) for data collected during two flights in the ARCTAS campaign. The scatter at low concentrations arises predominantly from noise, rather than mass contributions from surrounding ions.

10 Figure S2. Scatter plot showing the correlation between the integrated mass at m/z 73 and
60 for data collected during two flights in the ARCTAS campaign and for the SOA and
primary BBOA data from the AMS database. The signals are linearly correlated, but the
lower loadings at m/z 73 introduce substantial scatter into at low concentrations. Linear fits
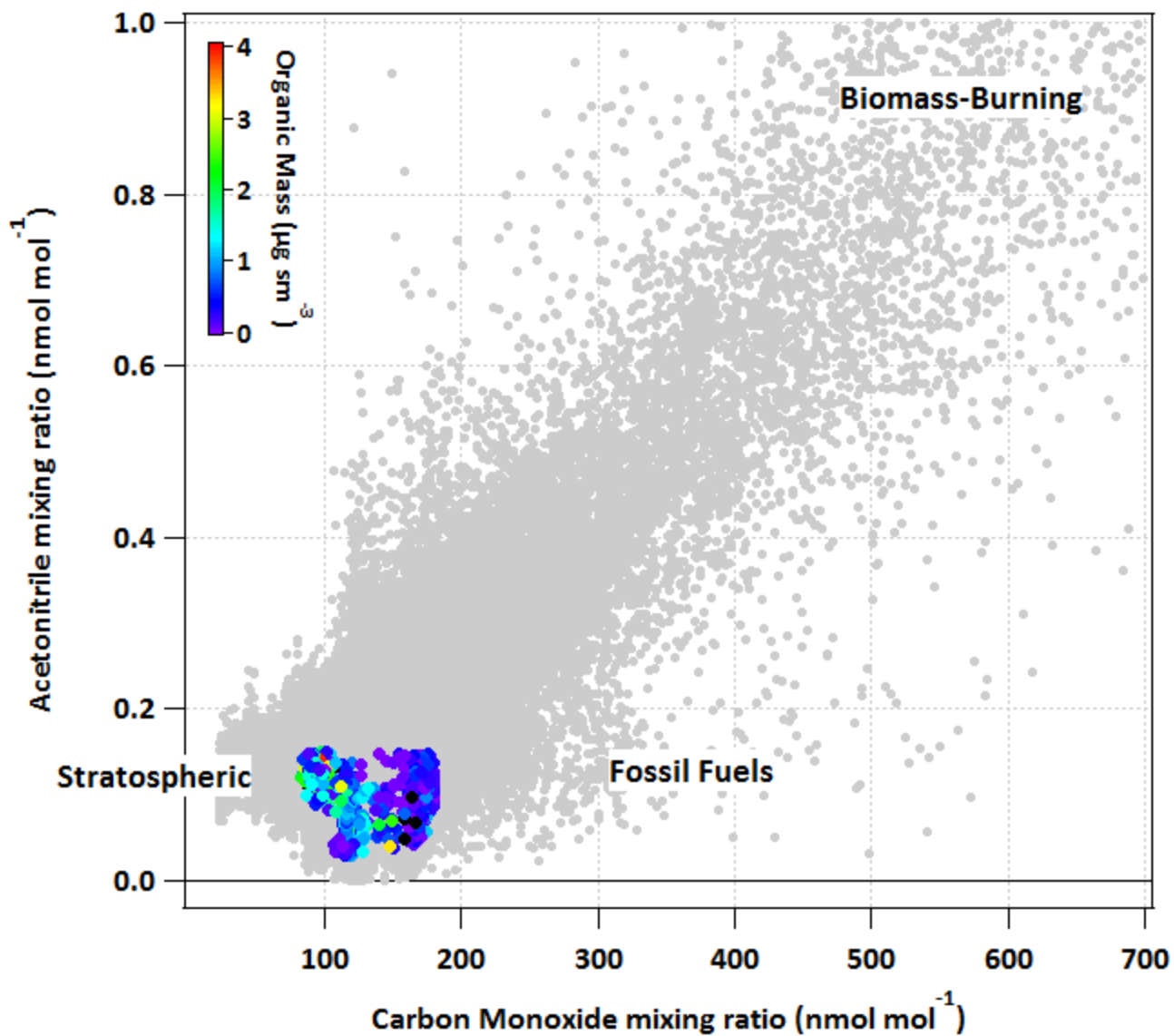to the ARCTAS data show negligible intercepts and slopes of ~0.59.

15

Figure S3. Scatter plot of the mixing ratios of gas-phase acetonitrile vs. carbon monoxide for all flights during the ARCTAS campaign, as measured by the PTR-MS and DACOM instruments, respectively. The coloured points represent those remaining after applying the background selection masks discussed in the text. These points best represent aged tropospheric air.
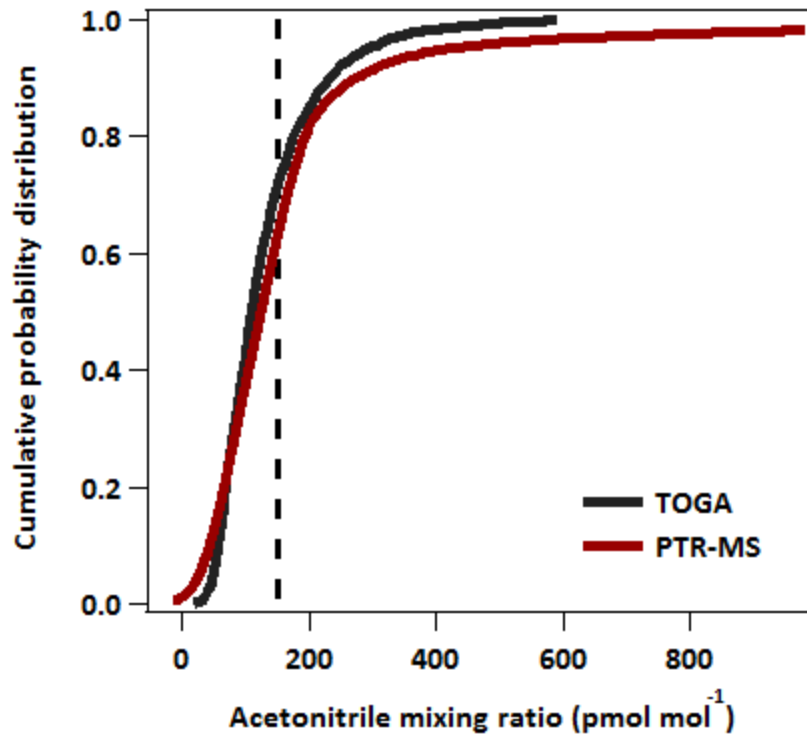
25 Figure S4. Cumulative probability distribution functions for the acetonitrile mixing ratio measured with two instruments for all data during the ARCTAS campaign. The background mask value from this study of 160 pmol mol^{-1} is indicated by the dashed line; the marked increase in concentrations associated with BB plumes in the upper quartile of the measurements lies above this value.
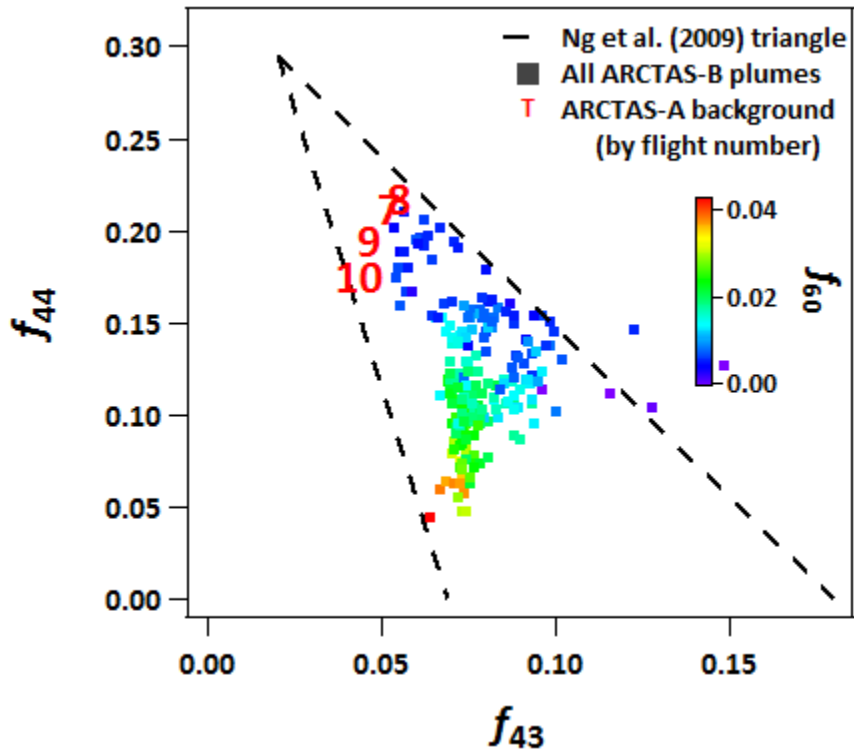
30

Figure S5. Comparison of f44 vs. f43 for ARCTAS Arctic background data, and each of the ARCTAS BB plumes categorised by Hecobian et al. (2011). The plume data are coloured by f_{60}. The dashed lines represent the ranges observed in field data (Ng et al., 2010); ambient data is observed to move towards the upper left corner under the influence of atmospheric processing.

35

5

10